

## Generation of a difference harmonic in a biased superlattice

A. V. Korovin,<sup>1</sup> F. T. Vasko,<sup>1,2</sup> and V. V. Mitin<sup>2</sup>

<sup>1</sup>*Institute of Semiconductor Physics, NAS of Ukraine, Kiev 252650, Ukraine*

<sup>2</sup>*Department of Electrical and Computer Engineering, Wayne State University, Detroit, Michigan 48202*

(Received 8 November 1999; revised manuscript received 31 January 2000)

We calculate the difference-harmonic susceptibility of a superlattice subject to uniform electric field, where generation of the difference harmonic is caused by interband transitions between hole and electron states. Both the electron and hole states are considered in the framework of the Kane model with parabolic dispersion laws. The hole states are uncoupled while for the electron states we use the tight-binding approximation. We obtain numerical results for spectral dependencies of the susceptibility under the double-resonant generation conditions, and discuss the efficiency of the double-frequency transformation of near-IR pump signal into THz radiation and modifications of the obtained nonlinear response with variation of the electric-field magnitude.

### I. INTRODUCTION

The second-order responses of various nonsymmetric semiconductor structures to high-frequency electro-magnetic field have been intensively studied over the past decade. The second-harmonic generation has been achieved by employing interband transitions of near-surface electrons and intersubband transitions of electrons in nonsymmetric heterostructures (see Refs. 1 and 2, respectively). Recently, new mechanisms of the difference-harmonic generation have come into existence, such as intersubband transitions of electrons in tunnel-coupled heterostructures (both experimental data<sup>3</sup> and theoretical considerations<sup>4,5</sup> have been published) and electron transitions in quantized metallic films.<sup>6</sup> To the best of our knowledge, the difference-harmonic generation due to interband transitions in nonsymmetric heterostructure has not yet been considered. In the present paper, we examine this possibility for an undoped superlattice subject to uniform electric field (biased superlattice, BSL). We also discuss numerical results for the efficiency of the process under consideration.

The scheme of two-frequency excitation of a BSL with the photon energies  $\hbar\omega_1$  and  $\hbar\omega_2$  is shown in Fig. 1. We have performed the calculation of the different-harmonic susceptibility in BSL for the case of weakly coupled SL, where the tight-binding approximation is valid for the low-energy electron states, while the hole states are assumed to be uncoupled. Based on the Kane model with parabolic dispersion laws,<sup>2,7</sup> we have calculated the interband transitions and analyze the spectral dependencies of susceptibility under the double-resonant conditions.

Both spectral and bias-voltage dependencies of the susceptibility occur to be sharp nonmonotonic functions of the difference between the energy of the pumping photons and the level-splitting energy (the last factor is determined by both the bias voltage and the value of the tunnel-coupling matrix element). The absolute magnitude of the susceptibility, which describes different-harmonic generation for typical parameters of GaAs/Al<sub>x</sub>Ga<sub>1-x</sub>As-based SL, is on several orders of magnitude greater than the magnitude of the second-order response for both the near-surface electron

states of bulk GaAs (Ref. 8) and the quantized electron states in heterostructures.<sup>9</sup>

Note that the system under consideration is of interest as a THz emitter among other cases that are actively investigated now: different modifications of quantum cascade laser,<sup>10</sup> transient oscillations under ultrafast optical pump,<sup>11,12</sup> and far-infrared emission from electrically driven BSL.<sup>13</sup> Therefore, we also add a brief electro-dynamical discussion to the efficiency of transformation of the near-IR pump into THz signal.

The paper is organized as follows. In Sec. II we transform the general expression of the third-order susceptibility tensor, using the tight-binding electron states and the uncoupled hole states for the BSL under consideration. The numerical results for the susceptibility versus the photon energies  $\hbar\omega_1$ ,  $\hbar\omega_2$  and versus the electric-field magnitude are presented in Sec. III. The discussion of the assumptions used and the

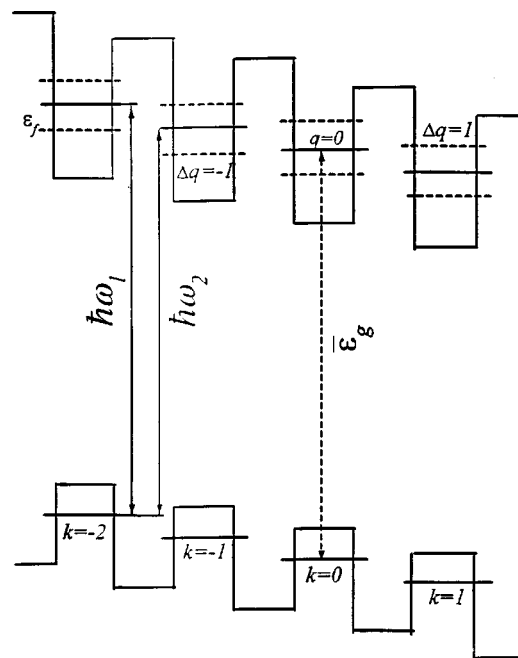


FIG. 1. The energy diagram of a biased superlattice being pumped by two beams with the photon energies  $\hbar\omega_1$  and  $\hbar\omega_2$ .

comparison with the other methods of THz generation are given in the concluding section.

## II. INTERBAND SUSCEPTIBILITY

The general expression for the nonlinear susceptibility tensor of the third order,  $\chi_{\alpha\beta\gamma}$ , which describes the generation of the difference harmonic, is written here on the basis of the eigenstates problem  $\hat{h}|\nu\rangle = \varepsilon_\nu|\nu\rangle$ , where  $\hat{h}$  is the Kane Hamiltonian for SL (see Refs. 2 and 7),  $|\nu\rangle$  and  $\varepsilon_\nu$  are the eigenstate vector and the energy in SL under a uniform electric field, respectively. For the undoped structure, we take into account only the transitions between occupied  $v$ -band states,  $|\nu_v\rangle$ , and empty  $c$ -band states,  $|\nu_c\rangle$ . Consideration of the second-order response on perturbation  $(ie/\omega_{1,2})\mathbf{E}_{1,2}\hat{\mathbf{v}}$ , where  $\mathbf{E}_{1,2}$  are the strengths of electric field of the first and the second beams and  $\hat{\mathbf{v}}$  is velocity operator, gives us the susceptibility,  $\chi_{\alpha\beta\gamma}(\omega_1, \omega_2)$ , in the form

$$\chi_{\alpha\beta\gamma}(\omega_1, \omega_2) = \frac{i|e|^3}{\Delta\omega\omega_1\omega_2L^3} \sum_{\nu_c\nu_v\nu} \left[ \Theta_{\alpha\beta}(\nu_c, \nu_v, \nu) \times \frac{\langle \nu_v | \hat{v}_\gamma | \nu_c \rangle}{\varepsilon_{\nu_v} - \varepsilon_{\nu_c} + \hbar\omega_2 - i\lambda} - \Theta_{\alpha\gamma}(\nu_v, \nu_c, \nu) \frac{\langle \nu_c | \hat{v}_\beta | \nu_v \rangle}{\varepsilon_{\nu_c} - \varepsilon_{\nu_v} - \hbar\omega_1 - i\lambda} \right]. \quad (1)$$

Here,  $\Delta\omega = \omega_1 - \omega_2$  is the difference frequency,  $\langle \nu_v | \hat{v}_\alpha | \nu_c \rangle$  is the velocity matrix element,  $\alpha, \beta, \gamma$  are the Cartesian coordinate indexes, and  $L^3$  is the normalization volume. Besides the summations over the states  $|\nu_c\rangle$  and  $|\nu_v\rangle$ , Eq. (1) contains the intermediate summation over  $\nu$ , which includes all the states. The  $\Delta\omega$ -dependent factor,  $\Theta_{\alpha\beta}$ , has the form

$$\Theta_{\alpha\beta}(\nu, \nu', \nu'') = \frac{\langle \nu | \hat{v}_\alpha | \nu'' \rangle \langle \nu'' | \hat{v}_\beta | \nu' \rangle}{\varepsilon_{\nu''} - \varepsilon_\nu - \hbar\Delta\omega - i\lambda} - \frac{\langle \nu | \hat{v}_\beta | \nu'' \rangle \langle \nu'' | \hat{v}_\alpha | \nu' \rangle}{\varepsilon_{\nu''} - \varepsilon_{\nu'} - \hbar\Delta\omega - i\lambda}, \quad (2)$$

where the transition broadening  $\lambda$  is a phenomenological parameter that is supposed to be independent of the quantum numbers, i.e., the broadening is the same for all the transitions. Restricting the sum in Eq. (1) to the resonant contributions only, we transform this equation into

$$\chi_{\alpha\beta\gamma}(\omega_1, \omega_2) = \frac{i|e|^3}{\Delta\omega\omega_1\omega_2L^3} \times \sum_{\nu_v\nu_c\nu_c'} \frac{\langle \nu_c' | \hat{v}_\alpha | \nu_c \rangle \langle \nu_c | \hat{v}_\beta | \nu_v \rangle \langle \nu_v | \hat{v}_\gamma | \nu_c' \rangle}{\varepsilon_{\nu_c} - \varepsilon_{\nu_c'} - \hbar\Delta\omega - i\lambda} \times \{ (\varepsilon_{\nu_c} - \varepsilon_{\nu_v} - \hbar\omega_1 - i\lambda)^{-1} - (\varepsilon_{\nu_c'} - \varepsilon_{\nu_v} - \hbar\omega_2 + i\lambda)^{-1} \}. \quad (3)$$

Since the problem is translation invariant for any in-plane direction, all the velocity matrix elements in Eq. (3) are diagonal over two-dimensional (2D) momentum,  $\mathbf{p}$ . The last multiplier in Eq. (3) depends on the momentum only in the case of parabolic dispersion law. For the near-edge interband transitions, which are only essential in Eq. (3), both  $cv$  and  $cc$  matrix elements are diagonal with respect to the spin numbers. Thus, the summation in Eq. (3) includes the integration over  $\mathbf{p}$  and the summation over the spin numbers,  $\sigma = \pm 1$ . The electron motion and the hole motion along the growth axis are characterized by the discrete quantum numbers  $k$  and  $q$ , respectively (see below).

The envelope function for the uncoupled hole states is written as  $\varphi_{z-kl}^{(v)}$  (cf. the discussion of assumptions in Sec. IV), where  $\varphi_z^{(v)}$  is the orbital of the hole ground state in the quantum well centered at  $z=0$ ,  $k$  is the number of quantum well, and  $l$  is the period of SL. The energy of the  $k$ th level is  $\varepsilon_k^{(v)} = -\bar{\varepsilon}_g - k\varepsilon_f$ ,  $\varepsilon_f = |e|F_\perp l$  being the level-splitting energy under the transverse electric-field magnitude  $F_\perp$  and  $\bar{\varepsilon}_g$  being the interband gap, which includes the electron and hole confinement effects. Taking into account the in-plane kinetic energy of the holes, we obtain the hole dispersion law in Eq. (3) in the form  $\varepsilon_{kp}^{(v)} = \varepsilon_k^{(v)} - p^2/(2m_h)$ . Here,  $m_h$  is the in-plane hole mass. This mass is essentially smaller than the bulk heavy-hole mass, due to the heavy-hole-light-hole mixing effect.

The  $c$ -band envelope function is written as a superposition  $\psi_{qz}^{(c)} = \sum_r \Psi_r^{(q)} \varphi_{z-rl}^{(c)}$ . Here,  $\varphi_z^{(c)}$  is the orbital of the electron ground state in the quantum well centered at  $z=0$  and  $r = 0, \pm 1, \pm 2, \dots$  because the BSL under consideration is supposed to be infinite in both directions. The column vector  $\Psi^{(q)}$  is determined by the eigenstates problem  $\hat{h}^{(SL)}\Psi^{(q)} = \varepsilon_q^{(c)}\Psi^{(q)}$ , where the matrix Hamiltonian of the BSL is written as

$$h_{rr'}^{(SL)} = T(\delta_{rr'-1} - \delta_{rr'+1}) + \delta_{rr'}\varepsilon_f, \quad (4)$$

$T$  is the tunnel matrix element for weakly coupled  $c$ -band states in adjacent quantum wells. The resulting wave function takes the form

$$\psi_{qz}^{(c)} = N_q \sum_r J_{q-r} \left( \frac{2T}{\varepsilon_f} \right) \varphi_{z-rl}^{(c)}, \quad (5)$$

where  $J_r(z)$  is the  $r$ th-order Bessel function and  $N_q = \pm 1$  is the normalization of the wave function [ $N_q^{-2} = \sum_{r=-\infty}^{\infty} J_{q-r}^2(2T/\varepsilon_f) = 1$ ]. The corresponding energy is  $q\varepsilon_f$ ,  $q = 0, \pm 1, \pm 2, \dots$ , so that the electron dispersion law is as  $\varepsilon_{qp}^{(c)} = q\varepsilon_f + p^2/(2m_c)$ , where  $m_c$  is the  $c$ -band effective mass.

The interband matrix elements of velocity in Eq. (3) are expressed through the overlap factor  $I_{k,q} = \int dz \varphi_{z-kl}^{(v)} \psi_{qz}^{(c)}$ , according to Ref. 2,

$$\langle k\sigma | \hat{v}_x | q\sigma \rangle = \frac{\mathcal{P}}{\sqrt{2}} I_{k,q}, \quad \langle k\sigma | \hat{v}_y | q\sigma \rangle = \sigma \frac{\mathcal{P}}{i\sqrt{2}} I_{k,q}, \quad (6)$$

where  $\mathcal{P}$  is the Kane velocity, and the  $z$  component of the interband velocity is zero. Neglecting the weak tunneling for the hole and electron ground states, we obtain the overlap

factor in the form  $I_{k,q} \approx N_q J_{q-k}(2T/\varepsilon_f)$ . Using the wave function of Eq. (5), we transform the intraband matrix element in Eq. (3) as follows:

$$\begin{aligned} \langle q' | \hat{v}_z | q \rangle &\approx i \frac{\varepsilon_f l}{\hbar} N_{q'} N_q \sum_{k=-\infty}^{\infty} k J_{q'-k} \left( \frac{2T}{\varepsilon_f} \right) J_{q-k} \left( \frac{2T}{\varepsilon_f} \right) \\ &= \pm \frac{i T l}{\hbar} N_{q'} N_q \delta_{q,q' \pm 1}. \end{aligned} \quad (7)$$

The right-hand side of this equality has been obtained upon the sum transformation based on the identity  $\sum_{k=-\infty}^{\infty} J_k(x) J_{k+s}(x) = \delta_{s,0}$ . The  $x$  and  $y$  components of the interband velocity are proportional to  $\delta_{q'q}$ . Thus, under the resonance approximation, these contributions drop out of the sum in Eq. (3). Using the matrix elements of Eq. (7), we rewrite the nonzero components of the susceptibility tensor  $\chi_{z\beta\gamma} = \chi_{z\gamma\beta}$  as

$$\begin{aligned} \chi_{z\beta\gamma}(\omega_1, \omega_2) &= \frac{|e|^3}{\Delta\omega\omega_1\omega_2 L^3} \\ &\times \sum_{\sigma p} \sum_{k q q'} \frac{\langle q' | \hat{v}_z | q \rangle \langle k | \hat{v}_\beta | q \rangle^* \langle k | \hat{v}_\gamma | q' \rangle}{\varepsilon_{qp}^{(c)} - \varepsilon_{q'p}^{(c)} - \hbar\Delta\omega - i\lambda} \\ &\times \{ (\varepsilon_{qp}^{(c)} - \varepsilon_{kp}^{(v)} - \hbar\omega_1 - i\lambda)^{-1} \\ &- (\varepsilon_{q'p}^{(c)} - \varepsilon_{kp}^{(v)} - \hbar\omega_2 + i\lambda)^{-1} \}, \end{aligned} \quad (8)$$

where  $\beta$  and  $\gamma$  are the in-plane indexes. The system under consideration is in-plane isotropic, so that  $\chi_{zxy} = \chi_{zyx} = 0$  [upon substitution of the matrix elements (6) in Eq. (8), we obtain  $\sum_{\sigma} \sigma = 0$ ] and  $\chi_{zxx} = \chi_{zyy} \equiv \chi_{\perp\parallel}$ . Substituting the matrix elements of Eqs. (6) and (7) in Eq. (8) and performing the summation over  $k$  (which gives us the normalization length along SL, according to  $\sum_{\kappa} l = L$ ), we obtain

$$\begin{aligned} \chi_{\perp\parallel}(\omega_1, \omega_2) &= \frac{|e|^3 \mathcal{P}^2 T}{\hbar \Delta\omega \omega_1 \omega_2} \int \frac{d\mathbf{p}}{(2\pi\hbar)^2} \\ &\times \sum_{\Delta q = \pm 1} \sum_{k-q} \frac{\Delta q J_{q-k}(2T/\varepsilon_f) J_{q-k-\Delta q}(2T/\varepsilon_f)}{\Delta q \varepsilon_f - \hbar\Delta\omega - i\lambda} \\ &\times \{ (\varepsilon_{(q-\Delta q)p}^{(c)} - \varepsilon_{kp}^{(v)} - \hbar\omega_2 + i\lambda)^{-1} \\ &- (\varepsilon_{qp}^{(c)} - \varepsilon_{kp}^{(v)} - \hbar\omega_1 - i\lambda)^{-1} \}. \end{aligned} \quad (9)$$

Here,  $\Delta q$  is restricted by the condition  $\Delta q = \pm 1$ , due to the selection rule in Eq. (7). The denominators in Eq. (9) contain the reduced dispersion law  $\varepsilon_{qp}^{(c)} - \varepsilon_{kp}^{(v)} = \bar{\varepsilon}_g + (q-k)\varepsilon_f + p^2/(2\mu)$ ;  $\mu = (1/m_c + 1/m_h)^{-1}$  being the reduced effective mass. The integral over the momentum plane in Eq. (9) can be expressed through the complex logarithm.

Finally, the expression for the susceptibility tensor is transformed into

$$\chi_{\perp\parallel}(\omega_1, \omega_2) = \frac{|e|^3 \mathcal{P}^2 T \rho_{2D}}{2\hbar \Delta\omega \omega_1 \omega_2} \frac{F(\delta\varepsilon, \hbar\Delta\omega)}{(\Delta q \varepsilon_f - \hbar\Delta\omega - i\lambda)}, \quad (10)$$

where  $\rho_{2D} = \mu/(\pi\hbar^2)$  is the reduced 2D density of states and  $\delta\varepsilon = \bar{\varepsilon}_g - \hbar(\omega_1 + \omega_2)/2$  is the detuning energy. The multiparameter function  $F(\delta\varepsilon, \hbar\Delta\omega)$  is given as

$$\begin{aligned} F(\delta\varepsilon, \hbar\Delta\omega) &= \sum_{q\Delta q} J_q \left( \frac{2T}{\varepsilon_f} \right) J_{q-\Delta q} \left( \frac{2T}{\varepsilon_f} \right) \\ &\times \left\{ \ln \sqrt{\frac{(\delta\varepsilon + q\varepsilon_f - \hbar\Delta\omega/2)^2 + \lambda^2}{(\delta\varepsilon + [q - \Delta q]\varepsilon_f + \hbar\Delta\omega/2)^2 + \lambda^2}} \right. \\ &+ i \left[ \arctan \left( \frac{\delta\varepsilon + q\varepsilon_f - \hbar\Delta\omega/2}{\lambda} \right) \right. \\ &\left. \left. + \arctan \left( \frac{\delta\varepsilon + [q - \Delta q]\varepsilon_f + \hbar\Delta\omega/2}{\lambda} \right) \right] \right\}. \end{aligned} \quad (11)$$

The contribution with  $\Delta q = \text{sgn}(\Delta\omega)$  is essential only for the double-resonance condition [the term with  $\Delta q = -\text{sgn}(\Delta\omega)$  occurs to be nonresonant]. Note, that  $F(\delta\varepsilon, \hbar\Delta\omega)$  is the even function with respect to  $\delta\varepsilon$ , i.e.,  $F(-\delta\varepsilon, \hbar\Delta\omega) = F(\delta\varepsilon, \hbar\Delta\omega)$ .

### III. NUMERICAL RESULTS

In this section, we obtain the spectral dependencies of the susceptibility (10) and examine the modifications of  $\chi_{\perp\parallel}$  under bias voltage variations. The numerical results have been obtained for GaAs/Al<sub>0.3</sub>Ga<sub>0.7</sub>As SL with the following characteristics: the quantum well (QW) layer width is 5 nm and the barrier layer width is 4 nm. We also have used the interband gap  $\bar{\varepsilon}_g$  that includes confinement effects in the hard wall QW approximation and  $\mu = 0.04m_0$ , where  $m_0$  is the free electron mass. The in-plane hole mass  $m_h \approx 0.09m_0$  have been taken from Ref. 14.

The absolute value of the susceptibility,  $|\chi_{\perp\parallel}|$ , its real part  $\text{Re}\chi_{\perp\parallel}$ , and its imaginary part  $\text{Im}\chi_{\perp\parallel}$ , are shown in Fig. 2, as functions of  $\delta\varepsilon$  and  $\hbar\Delta\omega$ . We put the broadening value  $\lambda = 1$  meV and the splitting energy  $\varepsilon_f = 10$  meV, which corresponds to the transverse electric field magnitude of 11.1 kV/cm. The obtained spectra are symmetric with respect to  $\delta\varepsilon$ ; the results are plotted for  $\delta\varepsilon > 0$  and  $\hbar\Delta\omega > 0$ , because we assume  $\omega_1 > \omega_2$ . Since the divergence of  $\chi_{\perp\parallel}$  at  $\Delta\omega \rightarrow 0$  is inessential,<sup>1</sup> we have obtained the spectral dependencies, starting with the difference photon energy 2.5 meV.

The spectral dependencies of both Fig. 2(a) and Fig. 2(b) show the resonant maximum at  $\hbar\Delta\omega \approx \varepsilon_f$ , under zero-detuning energy condition  $\delta\varepsilon = 0$ . The increase of  $\lambda$  suppresses this maximum, as shown in Fig. 3, where the peak value of  $\chi_{\perp\parallel}$  appears to be three times smaller, for  $\lambda = 2.5$  meV. However, the second-order nonlinearity for the system under consideration is substantially greater than both difference-harmonic and second-harmonic susceptibilities for bulk materials (cf. Refs. 15 and 8). The obtained susceptibility is also greater than the second-harmonic susceptibility in biased SL (Ref. 16) while the difference-harmonic susceptibility is comparable with that for the tunnel-coupled wells,<sup>3</sup> in spite of the fact that the energies  $\hbar\omega_{1,2}$  are substantially greater than those used in Ref. 3.

We have considered the near-resonant region  $\hbar\Delta\omega \approx \varepsilon_f$  in

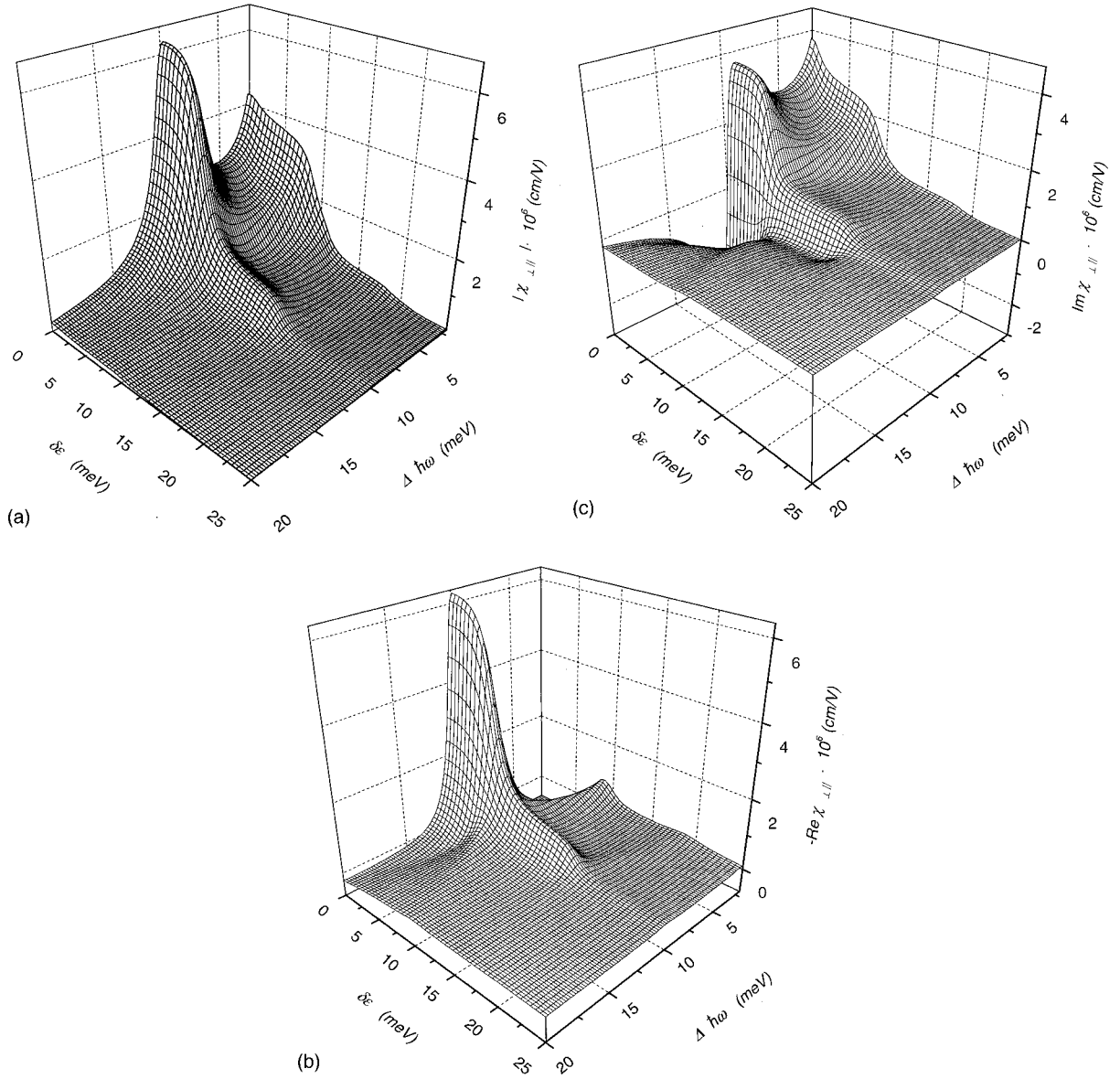


FIG. 2.  $|\chi_{\pm||}|$  (a),  $\text{Re}\chi_{\pm||}$  (b), and  $\text{Im}\chi_{\pm||}$  (c) versus the detuning energy  $\delta\varepsilon$  and the difference energy  $\hbar\Delta\omega$ ; the splitting energy is taken  $\varepsilon_f=10$  meV, the transition broadening  $\lambda=1$  meV.

more detail, and analyzed the dependencies of the susceptibility on the detuning energy and on the bias voltage. Note that the imaginary part of the susceptibility equals zero at the resonance. Making use of the resonant condition, we transform the expressions (10) and (11) into

$$\begin{aligned} \chi_{\pm||}(\delta\varepsilon) = & \frac{-|e|^3 \mathcal{P}^2 T \rho_{2D}}{\lambda \varepsilon_f \omega_1 \omega_2} \\ & \times \sum_q J_q\left(\frac{2T}{\varepsilon_f}\right) J_{q-1}\left(\frac{2T}{\varepsilon_f}\right) \\ & \times \arctan\left(\frac{\delta\varepsilon + (q-1/2)\varepsilon_f}{\lambda}\right). \end{aligned} \quad (12)$$

This function is shown in Fig. 4 for different splitting energies; all the curves are of steplike form. These steps are due to interband transitions from  $v$  band to several subbands of  $c$  band having the same energy but different values of  $2D$

momentum. If the splitting energy is relatively large [i.e., the argument of the Bessel functions in Eq. (12) is small], the susceptibility is determined by the transitions between the subbands with  $q=0$  and  $\pm 1$  only. In this situation the susceptibility curve has just two steps. At small splitting energies (i.e., large arguments of the Bessel functions), the transitions between other adjacent subbands become also essential; thus, the number of the steps increases.

Figure 5 shows the dependencies of the absolute value of the susceptibility on the bias voltage (which determines the splitting energy), at different pump frequencies. These electric-field dependencies have maximums at the condition  $\hbar\Delta\omega \approx \varepsilon_f$  and weakly steplike form in the low-field range. These steps are due to the transitions between nonadjacent subbands of the  $c$  band; the contribution of such transitions is comparatively small.

To estimate the intensity of the THz signal generated by the down-conversion process under consideration, we have calculated the THz flux along the SL plane (see the Appen-

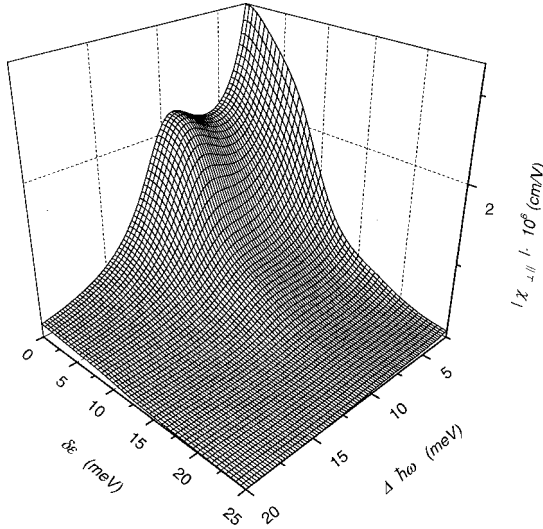


FIG. 3. The same as in Fig. 2(a), for the transition broadening  $\lambda = 2.5$  meV.

dix for details). The numerical results are obtained for the 500-period SL of the total thickness  $d \approx 5 \times 10^{-4}$  cm, under the pump intensity  $1.7$  kW/cm<sup>2</sup>, which corresponds to  $E_{1,2} \approx 0.3$  kV/cm. We assume that the two IR beams impinge on the sample at the angles  $64^\circ$  and  $60^\circ$ , so that the characteristic scale of the electric field localization in Eq. (A1) is  $\overline{\Delta k}^{-1} \approx d$ . Then, the intensity of the total energy flux along SL, introduced by Eqs. (A5) and (A6), is estimated as  $\overline{S} \approx 2 \times 10^{-7}$  W/cm. Thus, the power propagating along a SL strip of  $0.1$  cm width is equal to  $20$  nW. This value is  $30$  times greater than the result obtained in Ref. 3.

The output power increasing with the pump intensity as  $(E_1 E_2)^2$ , at  $E_{1,2} \sim 3$  kV/cm (which corresponds to the flux  $170$  kW/cm<sup>2</sup>) we obtain the THz signal power of about  $0.2$  mW/cm. Thus, BSL can be used for effective down-conversion of a pulse IR pump into THz radiation.

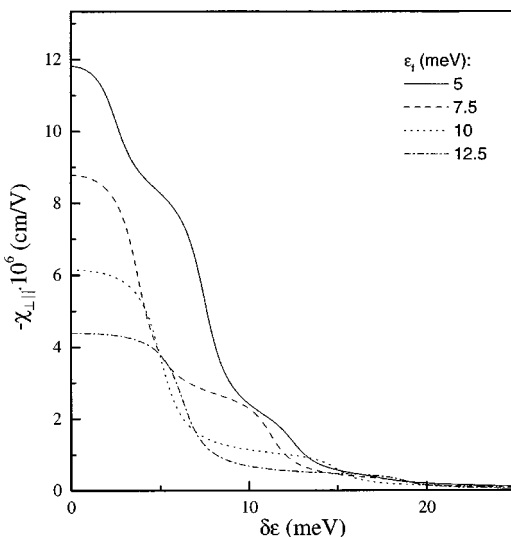


FIG. 4. The spectral dependencies of  $\chi_{\perp\parallel}$  as functions of the detuning energy, at  $\hbar\Delta\omega \approx \varepsilon_f$  and several splitting energies ( $\lambda = 1$  meV).

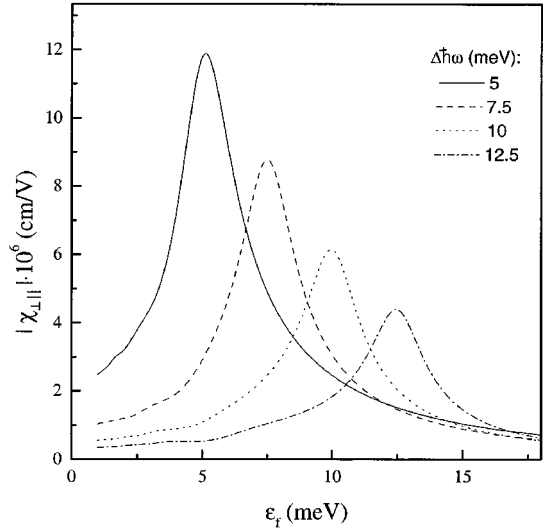


FIG. 5. The electric-field dependencies of  $|\chi_{\perp\parallel}|$  as functions of the splitting energy  $\varepsilon_f = |e|F_{\perp}l$  at  $\delta\varepsilon = 0$ ,  $\lambda = 1$  meV, and several values of  $\hbar\Delta\omega$ .

#### IV. CONCLUDING REMARKS

In this paper, we have obtained and analyzed the difference harmonic susceptibility,  $\chi_{\perp\parallel}$ , of a based superlattice. Both spectral and bias-voltage dependencies of  $\chi_{\perp\parallel}$  have been obtained, and the double-resonant enhancement of  $\chi_{\perp\parallel}$  has been demonstrated for  $\hbar(\omega_1 + \omega_2)/2$  close to  $\overline{\varepsilon}_g$  and  $\hbar|\Delta\omega|$  close to  $\varepsilon_f$ . The typical values of the susceptibility are a few times to an order of magnitude larger than those obtained for other mechanisms in Refs. 8, 9, 15, and 16, so that the efficiency of transformation of near-IR pump into THz signal appears to be noticeable.

Let us discuss the main assumptions we used in our calculations. The phenomenological description of the broadening of intersubband and interband transitions is generally accepted (see Ref. 1). The additional assumption of the broadening energy  $\lambda$  being the same for all the transitions does not substantially modify the shape of spectral dependencies and does not change the maximum value of  $\chi_{\perp\parallel}$  and presented numerical estimations will not change under more precise microscopical description of the relaxation processes. Due to significant broadening of the transitions in SL, we can also neglect all the exciton effects. As it is stated in Ref. 17 (see also referencies therein) the exciton effects are essential for more sensitive nonlinear effects, e.g., ultrafast four-wave mixing. The resonant character of the interband transitions allows us to use the parabolic dispersion laws for both the electrons and the holes. Since the heavy-hole underbarrier penetration is very weak, we consider the hole states as uncoupled. It is a satisfactory approximation for the parameters used in our numerical calculations (general consideration of the hole states in SL is presented in Ref. 7). For the same reason, the effects of heavy-hole–light-hole mixing on the tunneling are small enough and can be disregarded altogether (see the discussion on this matter in Ref. 18). The restrictions of the tight-binding approach for description of electron states are also well known<sup>2</sup> and errors are small in the case under consideration. Thus, all above listed approximations do not change either the character of spectral or electric-field

dependencies, nor the absolute values of susceptibility.

Next, look more closely at the comparison the scheme of THz emission suggested here and other methods discussed in literature. The complexity of the method under consideration is the cumbersome scheme of two-frequency optical pump. At the same time this method has a high enough efficiency of transformation and permits us to obtain monochromatic THz radiation in a continuous regimes. Although the spontaneous THz emission under intersubband transitions has been demonstrated recently,<sup>19,20</sup> the quantum cascade laser still remains to be unrealized for the THz spectral region. As for the different methods of THz emission under ultrafast optical pump,<sup>11,12</sup> some are more complicated than the method under consideration and such schemes permit us only to obtain ultrashort THz pulses with wide spectral characteristics.

To conclude, the obtained results convincingly demonstrate that the difference-harmonic response of biased superlattices in the situation of double resonance is a promising method of efficient THz emission due to down-conversion of intense two-color pumping.

#### ACKNOWLEDGMENTS

This work was supported by the NSF and by the JPL.

#### APPENDIX

Here, we discuss the efficiency of the transformation of interband pump into the THz signal, providing the specific geometry of the problem. We consider two IR beams with the incidence angles of  $\theta_1$  and  $\theta_2$  ( $\theta_1 \approx \theta_2$ ). They excite the interband transitions in the biased SL of total width  $d$ , placed into media with dielectric primitivity  $\epsilon$ . The THz energy flux along an in-plane direction  $OX$  and distribution of THz field  $E_z \exp(i\Delta\omega t - i\Delta k x)$  are determined by the wave equation

$$\left[ \frac{d^2}{dz^2} - \overline{\Delta k^2} \right] E_z = \begin{cases} -4\pi(\Delta\omega/c)^2 P_\perp, & |z| < d/2 \\ 0, & |z| > d/2. \end{cases} \quad (\text{A1})$$

We consider only the case of localized mode in the dielectric waveguide formed by the BSL [ $\overline{\Delta k^2} \equiv \Delta k^2 - \epsilon(\Delta\omega/c)^2 > 0$ ]. The in-plane wave vector  $\Delta k$  is determined as

$$\Delta k = k_1 \sin \theta_1 - k_2 \sin \theta_2 \approx \sqrt{\epsilon \bar{\epsilon}_g} / (\hbar c) (\sin \theta_1 - \sin \theta_2); \quad (\text{A2})$$

the induced polarization  $P_\perp$  is expressed through the susceptibility of Eq. (10) according to the expression  $P_\perp = \chi_{\perp||}(\omega_1, \omega_2) E_1 E_2$ , where  $E_1$  and  $E_2$  are the electric field magnitudes of the first and the second beams.

The system of ordinary differential Eqs. (A1) is completed by the continuity boundary conditions for  $E_z$  and  $dE_z/dz$  at  $z = \pm d/2$  and with zero-field conditions at  $z \rightarrow \pm \infty$ . The straightforward solution of this problem give us the following distribution of the transverse electric field:

$$E_z = \bar{E} \begin{cases} 1 - e^{-\overline{\Delta k} d/2} \cosh(\overline{\Delta k} z), & |z| < d/2 \\ \sinh(\overline{\Delta k} d/2) e^{-\overline{\Delta k} z}, & z > d/2 \\ \sinh(\overline{\Delta k} d/2) e^{\overline{\Delta k} z}, & z < -d/2, \end{cases} \quad (\text{A3})$$

where the characteristic field  $\bar{E}$  is introduced by the expression

$$\bar{E} = 4\pi \left( \frac{\Delta\omega}{c\overline{\Delta k}} \right)^2 \bar{\chi} E_1 E_2. \quad (\text{A4})$$

To estimate the maximum efficiency of the transformation, we use in Eq. (A4) the peak value of the susceptibility  $\bar{\chi}$ , which is realized under double resonance conditions. The Poynting vector of the THz radiation along the  $OX$  axis is given as

$$\mathbf{S} = \frac{c^2}{2\pi\Delta\omega} \mathcal{J}[\mathbf{E} \times [\nabla \times \mathbf{E}]^*] = \frac{c^2 \Delta \mathbf{k}}{2\pi\Delta\omega} E_z^2. \quad (\text{A5})$$

Thus, in the case of the normal interband excitation ( $\Delta k = 0$ ), there is no in-plane THz flux at all. The total energy flux along the SL axis,  $\bar{S} = \int_{-\infty}^{\infty} dz S_z$ , is obtained from Eqs. (A3)–(A5) as

$$\bar{S} = \frac{c^2 \Delta k}{2\pi\Delta\omega} \int dz E_z^2 = \frac{c^2 \bar{E}^2}{\pi\Delta\omega} \frac{\Delta k}{\overline{\Delta k}} F(\overline{\Delta k} d/2), \quad (\text{A6})$$

where the dimensionless function  $F(y) = y - 3/4 + (y/2 + 3/4)e^{-y^2}$ . Note, that the dimensionality of  $\bar{S}$  is W/cm, while the Poynting vectors of the pumping beams  $S_{1,2} = c\sqrt{\epsilon} E_{1,2}^2 / (2\pi)$  are measured in W/cm<sup>2</sup>.

<sup>1</sup>R.W. Boyd, *Nonlinear Optics* (Academic, Boston, 1992); Y.R. Shen, *The Principles of Nonlinear Optics* (Wiley, New York, 1984).

<sup>2</sup>F.T. Vasko and A.V. Kuznetsov, *Electron States and Optical Transitions in Semiconductor Heterostructures* (Springer, New York, 1998).

<sup>3</sup>C. Sirtori, F. Capasso, J. Faist, L.N. Pfeiffer, and K.W. West, *Appl. Phys. Lett.* **65**, 445 (1994).

<sup>4</sup>J.B. Khurgin, B. Saif, and B. Seery, *Appl. Phys. Lett.* **73**, 13 (1998).

<sup>5</sup>M. Zaluzny, *J. Appl. Phys.* **78**, 2868 (1995).

<sup>6</sup>A.V. Korovin and F.T. Vasko, *Appl. Phys. B: Lasers Opt.* **68**, 355 (1999).

<sup>7</sup>D.L. Smith and C. Mailhot, *Rev. Mod. Phys.* **62**, 173 (1990).

<sup>8</sup>J.L.P. Hughes and J.E. Sipe, *Phys. Rev. B* **53**, 10 751 (1996).

<sup>9</sup>K.A. Shore, X. Chen, and P. Blood, *Prog. Quantum Electron.* **20**, 181 (1996); H. Kuwatsuka and H. Ishikawa, *Phys. Rev. B* **50**, 5323 (1994).

<sup>10</sup>F. Capasso, C. Gmachl, D.L. Sivco, and A.Y. Cho, *Phys. World* **12**, 27 (1999).

<sup>11</sup>K. Leo, *Semicond. Sci. Technol.* **13**, 249 (1998).

<sup>12</sup>A. Schülzgen, R. Binder, M.E. Donovan, M. Lindberg, K.

- Wundke, H.M. Gibbs, G. Khitrova, and N. Peyghambarian, *Phys. Rev. Lett.* **82**, 2346 (1999); E. Diez, R. Gómez-Alcalá, F. Domínguez-Adame, A. Sánchez, and G.P. Berman, *Phys. Rev. B* **58**, 1146 (1998).
- <sup>13</sup>J. Ulrich, R. Zobl, K. Unterrainer, G. Strasser, E. Gornik, K.D. Maranowski, and A.C. Gossard, *Appl. Phys. Lett.* **74**, 3158 (1999); M. Helm, P. England, E. Colas, F. DeRosa, and S.J. Allen, *Phys. Rev. Lett.* **63**, 74 (1989).
- <sup>14</sup>D.H. Huang and S.K. Lyo, *Phys. Rev. B* **59**, 7600 (1999).
- <sup>15</sup>D.W. Faries, K.A. Genning, P.L. Richards, and Y.R. Shen, *Phys. Rev.* **180**, 363 (1969).
- <sup>16</sup>W.W. Bewley, C.I. Felix, J.J. Plombon, M.S. Sherwin, M. Sundaram, P.F. Hopkins, and A.C. Gossard, *Phys. Rev. B* **48**, 2376 (1993).
- <sup>17</sup>Th. Östreich, K. Schönhammer, and L.J. Sham, *Phys. Rev. B* **58**, 12 920 (1998).
- <sup>18</sup>F.T. Vasko and O.E. Raichev, *Zh. Éksp. Teor. Fiz.* **104**, 3103 (1993) [*JETP* **77**, 452 (1993)]; F.T. Vasko and O.E. Raichev, *Fiz. Tekh. Poluprovodn.* **29**, 1579 (1995) [*Semiconductors* **29**, 822 (1995)].
- <sup>19</sup>M. Rochat, J. Faist, M. Beck, U. Oesterle, and M. Illegems, *Appl. Phys. Lett.* **73**, 3724 (1998).
- <sup>20</sup>B.S. Williams, B. Xu, Q. Hu, and M.R. Melloch, *Appl. Phys. Lett.* **75**, 2927 (1999).